NJC

PAPER

View Article Online
View Journal | View Issue



Cite this: *New J. Chem.*, 2018, **42**, 56



# The molecular design of cage metal complexes for biological applications: pathways of the synthesis, and X-ray structures of a series of new $N_2$-, $S_2$- and $O_2$-alicyclic iron(II) di- and tetrachloroclathrochelates†

Genrikh E. Zelinskii,[a] Alexander S. Belov,[a] Irina G. Belaya,[a] Anna V. Vologzhanina,[a] Valentin V. Novikov,[a] Oleg A. Varzatskii[b] and Yan Z. Voloshin *[ac]

The synthesis of new metal(II) di- and tetrahalogenoclathrochelates with apical functionalizing substituents as reactive macrobicyclic precursors is a key stage of the molecular design of cage metal complexes – prospective biological effectors. We found that the most convenient multistep synthetic pathway for their preparation includes (i) direct template condensation of a dihalogeno-α-dioxime with an appropriately functionalized boronic acid on the corresponding metal ion as a matrix, giving an apically functionalized metal hexahalogenoclathrochelate in a high yield; and (ii) its stepwise nucleophilic substitution with $S_2$-, $N_2$- or $O_2$-bis-nucleophiles, forming stable six-membered alicyclic ribbed fragments, thus allowing obtaining the corresponding apically functionalized di- and tetrahalogenoclathrochelates. The latter reaction of an iron(II) hexachloroclathrochelate with different $N_2$-, $S_2$- and $O_2$-bis-nucleophilic agents afforded chloroclathrochelate complexes with equivalent and non-equivalent alicyclic ribbed substituents, such as $N_2$-, $S_2$ or $O_2$-containing six-membered cycles. In the case of anionic forms of pyrocatechol and 1,2-ethanedithiol as $O_2$- and $S_2$-bis-nucleophiles, generated *in situ* in the presence of triethylamine, such substitution proceeds easily and in a high yield. In the case of anionic derivatives of ethylenediamine as $N_2$-bis-nucleophiles, only a mono-$N_2$-alicyclic iron(II) tetrachloroclathrochelate was obtained in a moderate yield. The $S_2$-alicyclic iron(II) tetrachloroclathrochelate underwent a further nucleophilic substitution of one of the two dichloroglyoximate fragments, giving its $N_2$, $S_2$-alicyclic dichloroclathrochelate derivative with three non-equivalent ribbed chelate fragments. The complexes obtained were characterized using elemental analysis, MALDI-TOF mass spectrometry, and IR, UV-vis, $^1$H and $^{13}$C{$^1$H} NMR spectroscopies, and by single crystal X-ray diffraction (XRD). As follows from XRD data for four $O_2$-, $S_2$- and $N_2$-ribbed-functionalized iron(II) clathrochelates, the geometry of their $FeN_6$-coordination polyhedra is intermediate between a trigonal prism and a trigonal antiprism. UV-vis spectra of these cage complexes are indicative of a dramatic redistribution of the electron density in a quasiaromatic clathrochelate framework caused by its ribbed functionalization with six-membered $O_2$-, $S_2$- and/or $N_2$-alicyclic substituent(s).

Received 18th August 2017,
Accepted 9th November 2017

DOI: 10.1039/c7nj03051g

rsc.li/njc

## Introduction

Several examples of efficient transcription inhibition by designed iron(II) cage and bis-cage complexes[1,2] have been previously reported[3–6] for a model *in vitro* system based on a T7 RNA polymerase (T7 RNAP). This small single-subunit polymerase is a convenient and reliable model in the search for transcription inhibitors[7] and these ribbed-functionalized clathrochelates and bis-clathrochelates have demonstrated structure- and concentration-dependent inhibition in its transcription assay. Their inhibition mode has been deduced[4] using experimental

[a] *Nesmeyanov Institute of Organoelement Compounds of the Russian Academy of Sciences, 119991 Moscow, Russia. E-mail: voloshin@ineos.ac.ru*
[b] *Vernadskii Institute of General and Inorganic Chemistry NASU, 03680, Kiev, Ukraine*
[c] *Kurnakov Institute of General and Inorganic Chemistry of the Russian Academy of Sciences, 119991, Moscow, Russia*

† Electronic supplementary information (ESI) available. CCDC 1433324–1433326. For ESI and crystallographic data in CIF or other electronic format see DOI: 10.1039/c7nj03051g

 

preincubation data and molecular docking calculations: the rigid and bulky three-dimensional inhibitor molecule is located in the same region of a supramolecular complex, formed by the macromolecules of T7 RNAP, matrix DNA and RNA synthesized – in the transcriptional "bubble" – and is involved in the intermolecular contacts with protein residues, as well as with DNA and RNA. The surfaces of DNA and RNA form the framework of the pocket for the inhibitor's binding, while the two structural elements of T7 RNAP interact with the ribbed phenyl substituents of a clathrochelate molecule, thus completing the formation of the above pocket. As a result, trapping of this macrobicyclic inhibitor occurred. So, the activity of such cage inhibitors is affected not only by a geometric complementarity between these clathrochelate guests and the above pockets as hosts, but also by the ability of the peripheral and terminal groups in their apical and ribbed substituents to form stable supramolecular bonds with hydrophobic and hydrophilic (polar) fragments of the biomacromolecules forming a hosting site. Moreover, such host–guest supramolecular binding depends not only on the hydrophilic–hydrophobic balance in an inhibitor cage molecule but also on the chemical nature of its peripheral and terminal groups: it is also affected by a spatial orientation of these groups within this pocket and, therefore, by their positions at a rigid quasiaromatic clathrochelate framework. Among the iron(II) clathrochelates and bis-clathrochelates, which have been tested in this model system to date, monoribbed-functionalized cage complexes (Scheme 1) with hydrophobic ribbed substituents in two of their three chelate fragments, with the third fragment of this type containing the functionalizing substituents with terminal biorelevant polar and H-bond donors (in particular carboxyl) terminal groups, have been previously recognized as the most efficient submicromolar inhibitors.[4,6] The same iron(II) cage complexes have recently been recognized[8] as efficient transcription inhibitors in the system of DNA polymerase. These leader cage and bis-cage inhibitors have been studied[9] for their binding to bovine serum albumin (BSA), β-lactoglobulin, lysozyme, and insulin using steady-state and time-resolved fluorescence spectroscopies. Quenching of the protein's fluorescence and a decrease in its excited state lifetime have been observed only in the case of BSA, thus suggesting the formation of strong supramolecular assemblies by these mono- and bis-clathrochelates with serum albumins, but not with other globular proteins.[9] These compounds have been also tested[10] as prospective antifibrillogenic agents in the *in vitro* system with insulin. They were found to substantially affect the kinetics of insulin fibrillization, thus reducing the amount of fibrils formed, decreasing their diameter and preventing the lateral aggregation of mature fibrils and the formation of superfibrillar clusters.[10] Very recently, based on *in vitro* studies, we found[11] that an iron(II) hexachloroclathrochelate exhibits substantial cytotoxicity and a high selectivity (as compared with normal cells) in human promyelocytic leukemia cells. Such toxicity is explained[11] by the ability of this electrophilic complex to increase the intracellular oxidative stress, caused by alkylation of glutathione, thus leading to the inhibition of the cellular antioxidative system, as well as by the catalytic generation of reactive oxygen species with partially alkylated clathrochelate products.

The previously elaborated most convenient pathway for the synthesis of monoribbed-functionalized iron and cobalt mono- and dihalogenoclathrochelates[12–16] is based on the condensation of the corresponding mono- or dihalogeno-α-dioxime with a macrocyclic metal bis-dioximate, the derivative of an aliphatic or aromatic α-dioxime, followed by chemical transformations of thus obtained mono- or dihalogenoclathrochelate precursors. However, this synthetic approach can be performed under vigorous reaction conditions only for several types of α-dioximes and only for fluoroboron-capped cage complexes. The bis-α-benzildioximate mono- and dihalogenoclathrochelates of this type have been recognized as the most suitable reactive macrobicyclic precursors of the above biological effectors: they easily undergo well-known classical organic reactions, such as *N*,*O*,*S*,*C*,*P*-nucleophilic substitution[12,13,17–22] (including cadmium-promoted reactions with low-active nucleophiles[21,22]), free-radical substitution,[23–28] copper-promoted cyanation,[29] electrophilic addition (for their amine derivatives[30,31]), and copper(0)- and copper(I)-promoted reactions of halogen exchange,[32] reductive homocoupling,[6,33] and hydrodehalogenation.[29,33] However, the apical functionalization of these fluoroboron-capped halogenoclathrochelate precursors, allowing tuning the physical properties of their macrobicyclic derivatives (in particular their solubility in water or biological media), and performing their efficient binding to a given biological target, is hardly possible (or even impossible). In this work, we aimed to elaborate the efficient synthetic strategies and procedures for a gram-scale synthesis of new iron(II) di- and tetrahalogenoclathrochelates as suitable macrobicyclic precursors for the molecular design of cage metal complexes (prospective biological effectors) and to study their structure and reactivity.

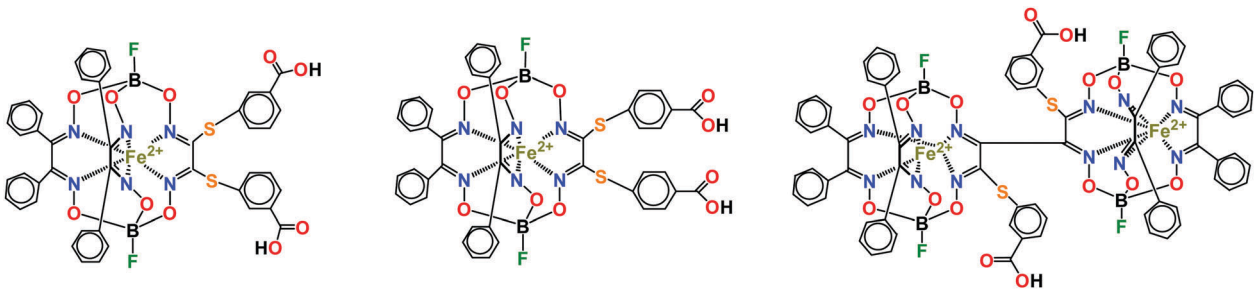

Scheme 1 The most efficient clathrochelate and bis-clathrochelate inhibitors in the transcription system of T7 RNAP.

# Experimental

The reagents used, triethylamine, pyrocatechol (Prch), 1,2-ethylenediamine, 1,2-ethanedithiol, sorbents and organic solvents were obtained commercially (SAF). The hexachloroclathrochelate **Fe(Cl$_2$Gm)$_3$(B*n*-C$_4$H$_9$)$_2$** (where Cl$_2$Gm$^{2-}$ is a dichloroglyoxime dianion) was prepared as described in ref. 17.

Analytical data (C, H, N contents) were obtained with a Carlo Erba model 1106 microanalyzer.

MALDI-TOF mass spectra were recorded with and without a matrix using a MALDI-TOF-MS Bruker Autoflex II (Bruker Daltonics) mass spectrometer in reflecto-mol mode. The ionization was induced by a UV-laser with a wavelength of 337 nm. The samples were applied to a nickel plate, and 2,5-dihydroxybenzoic acid was used as the matrix. The accuracy of measurements was 0.1%.

$^1$H and $^{13}$C NMR spectra were recorded from solutions in $CD_2Cl_2$, $CDCl_3$ and $CD_3OD$ with Bruker AMX-400 and Avance 600 spectrometers. The measurements were performed using the residual signals of these deuterated solvents.

UV-vis spectra of solutions in dichloromethane were recorded in the range 230–800 nm with a Varian Cary 50 spectrophotometer. The individual Gaussian components of these spectra were calculated using the Fityk program.[34]

## Synthesis

**Fe(*S*$_2$-Nx)(Cl$_2$Gm)$_2$(B*n*-C$_4$H$_9$)$_2$ (1).** This procedure was performed under pseudo-high dilution conditions. A solution of the complex **Fe(Cl$_2$Gm)$_3$(B*n*-C$_4$H$_9$)$_2$** (0.10 g, 0.15 mmol) in dichloromethane (30 ml), and a solution of 1,2-ethanedithiol (0.016 ml, 0.0141 mmol) and trimethylamine (0.364 ml, 3.6 mmol) in dichloromethane (30 ml) were simultaneously added dropwise to the stirring dichloromethane (100 ml) for 4 h. The reaction mixture was stirred for 24 h; the reaction course was monitored by TLC ($SiO_2$, eluent: dichloromethane–hexane 1 : 1 mixture). Then the reaction mixture was evaporated to dryness and the solid residue was extracted with benzene (5 ml). The extract was filtered, evaporated to dryness and the solid residue was extracted with a chloroform–hexane 3 : 1 mixture. The extract was flash-chromatographically separated on silica gel (30 mm layer; first eluent: hexane; second eluent: hexane–chloroform 2 : 1 mixture). The first elute was discarded; the second elute was filtered and evaporated to dryness and the solid residue was dried *in vacuo*. Yield: 0.072 g (70%). Anal. calc. (%) for $C_{16}Cl_4B_2O_6S_2H_{22}FeN_6$: C, 28.35; H, 3.27; N, 12.40. Found (%): C, 28.49; H, 3.45; N, 12.34. $^1$H NMR ($CD_2Cl_2$, $\delta$, ppm): 0.65 (t, 4H, $CH_2B$), 0.93 (t, 6H, $CH_3$), 1.40 (m, 8H, $(CH_2)_2$ (Bu)), 3.43 (s, 4H, $SCH_2$). $^{13}C\{^1H\}$ NMR ($CD_2Cl_2$, $\delta$, ppm): 14.53 (s, $CH_3$), 16.97 (br. s, $CH_2B$), 26.29, 26.69 (two s, $(CH_2)_2$ (Bu)), 28.94 (s, $SCH_2$), 129.40 (s, ClC═N), 144.89 (s, SC═N). MS (MALDI-TOF): *m*/*z*: 678 $[M]^{+\bullet}$. UV-vis ($CH_2Cl_2$): $\lambda_{max}$, nm ($\varepsilon \times 10^{-3}$, mol$^{-1}$ L cm$^{-1}$): 256 (5.5), 288 (3.0), 294 (5.8), 355 (1.6), 452 (10), 457 (6.9).

**Fe(*S*$_2$-Nx)$_2$(Cl$_2$Gm)(B*n*-C$_4$H$_9$)$_2$ (2).** This procedure was also performed under pseudo-high dilution conditions. A solution of the complex **Fe(Cl$_2$Gm)$_3$(B*n*-C$_4$H$_9$)$_2$** (0.20 g, 0.31 mmol) in dichloromethane (25 ml), and a solution of 1,2-ethanedithiol (0.060 g, 0.64 mmol) and trimethylamine (0.13 ml, 1.3 mmol) in dichloromethane (30 ml) were simultaneously added dropwise to the stirring dichloromethane (100 ml) for 4 h. The reaction mixture was stirred for 24 h; the reaction course was controlled by TLC ($SiO_2$, eluent: dichloromethane–hexane 1 : 1 mixture). Then the reaction mixture was evaporated to dryness and the solid residue was extracted with benzene (5 ml). The extract was filtered, evaporated to dryness and the product was extracted with a hexane–dichloromethane 2 : 1 mixture. The extract was flash-chromatographically separated on silica gel (70 mm layer, eluent: hexane–dichloromethane 2 : 1 mixture). The first elute was discarded; the second elute was filtered and evaporated to dryness and the solid residue was dried *in vacuo*. Yield: 0.068 g (33%). Anal. calc. (%) for $C_{18}Cl_2B_2O_6S_4H_{26}FeN_6$: C, 30.92; H, 3.75; N, 12.02. Found (%): C, 30.75; H, 3.78; N, 11.85. $^1$H NMR ($CD_2Cl_2$, $\delta$, ppm): 0.64 (t, 4H, $CH_2B$), 0.96 (t, 6H, $CH_3$), 1.42 (m, 8H, $(CH_2)_2$ (Bu)), 3.43 (s, 8H, $SCH_2$). $^{13}C\{^1H\}$ NMR ($CD_2Cl_2$, $\delta$, ppm): 14.55 (s, $CH_3$), 17.24 (br. s, $CH_2B$), 26.36, 26.92 (two s, $(CH_2)_2$ (Bu)), 28.93 (s, $SCH_2$), 127.67 (s, ClC═N), 143.16 (s, SC═N). MS (MALDI-TOF): *m*/*z*: 699 $[M]^+$. UV-vis ($CH_2Cl_2$): $\lambda_{max}$, nm ($\varepsilon \times 10^{-3}$, mol$^{-1}$ L cm$^{-1}$): 256 (13), 293 (11), 350 (3.6), 467 (7.5), 470 (18).

**Fe(*N*$_2$-Nx)(Cl$_2$Gm)$_2$(B*n*-C$_4$H$_9$)$_2$ (3).** This complex was obtained like the previous one except that ethylenediamine (0.111 ml, 0.15 mmol) was used instead of 1,2-ethanedithiol. Yield: 0.076 g (77%). Anal. calc. (%) for $C_{16}Cl_4B_2O_6N_8H_{24}Fe$: C, 29.85; H, 3.76; N, 17.41. Found (%): C, 29.78; H, 3.64; N, 17.27. $^1$H NMR ($CD_3OD$, $\delta$, ppm): 0.50 (t, 4H, $CH_2B$), 0.88 (t, 6H, $CH_3$), 1.34 (m, 8H, $(CH_2)_2$ (Bu)), 3.39 (s, 4H, $NCH_2$). $^{13}C\{^1H\}$ NMR ($CD_3OD$, $\delta$, ppm): 14.61 (s, $CH_3$), 27.07, 27.52 (two s, $(CH_2)_2$ (Bu)), 40.88 (s, $CH_2N$), 127.65 (s, ClC═N), 143.96 (s, NC═N). MS (MALDI-TOF): *m*/*z*: 644 $[M]^+$. UV-vis ($CH_2Cl_2$): $\lambda_{max}$, nm ($\varepsilon \times 10^{-3}$, mol$^{-1}$ L cm$^{-1}$): 256 (2.7), 277 (10), 360 (6.7), 418 (4.1), 487 (10), 597 (0.7).

**Fe(*N*$_2$-Nx)(*S*$_2$-Nx)(Cl$_2$Gm)(B*n*-C$_4$H$_9$)$_2$ (4).** Complex **1** (0.51 g, 0.75 mmol) was dissolved in dichloromethane (5 ml) under argon and a solution of ethylenediamine (0.103 ml, 1.5 mmol) in dichloromethane (1 ml) was added dropwise for 30 min to the stirring reaction mixture. The reaction mixture was stirred for 1 h; the reaction course was controlled by TLC ($SiO_2$, eluent: chloroform–hexane 1 : 1 mixture). Then ethylenediamine (0.103 ml, 1.5 mmol) was added to the reaction mixture (in three portions, during 3 h). Then the reaction mixture was evaporated to dryness, and the solid residue was extracted with benzene (5 ml). The extract was filtered, evaporated to dryness and the product was extracted with dichloromethane (2 ml). The extract was flash-chromatographically separated on silica gel (30 mm layer, first eluent: hexane–dichloromethane 1 : 1 mixture; second eluent: hexane–dichloromethane 1 : 2 mixture). The first elute was discarded; the second elute was filtered, evaporated to dryness and the solid residue was dried *in vacuo*. Yield: 0.41 g (81%). Anal. calc. (%) for $C_{18}Cl_2B_2O_6S_2H_{26}FeN_8$: C, 32.61; H, 3.95; N, 16.90. Found (%): C, 32.48; H, 4.11; N, 16.70. $^1$H NMR ($CD_2Cl_2$, $\delta$, ppm): 0.50 (t, 4H, $CH_2B$), 0.91 (t, 6H, $CH_3$), 1.35 (m, 8H, $(CH_2)_2$ (Bu)), 3.39 (s, 4H, $SCH_2$), 3.49 (s, 4H, $NCH_2$), 5.63 (s, 2H, NH). $^{13}C\{^1H\}$ NMR ($CD_2Cl_2$, $\delta$, ppm): 14.57 (s, $CH_3$), 17.79

 

(br. s, $CH_2B$), 26.55, 27.19 (two s, $(CH_2)_2$ (Bu)), 28.99 (s, $SCH_2$), 40.87 (s, $NCH_2$), 125.47 (s, ClC═N), 141.24, 141.48 (two s, SC═N + NC═N). MS (MALDI-TOF): *m*/*z*: 665 $[M]^+$. UV-vis ($CH_2Cl_2$): $\lambda_{max}$, nm ($\varepsilon \times 10^{-3}$, $mol^{-1}$ L $cm^{-1}$): 236 (13), 289 (4.2), 378 (3.6), 411 (0.3), 426 (1.9), 447 (2.4), 484 (4.2), 521 (3.8), 535 (1.0), 577 (0.4).

**Fe(PrchGm)$_3$(B*n*-C$_4$H$_9$)$_2$ (5).** The complex **Fe(Cl$_2$Gm)$_3$(B*n*-C$_4$H$_9$)$_2$** (0.30 g, 0.46 mmol) and pyrocatechol (0.31 g, 2.8 mmol) were dissolved/suspended in nitromethane (4 ml) under argon and a solution of triethylamine (0.46 ml, 3.3 mmol) in nitromethane (2 ml) was added. The reaction mixture was stirred at 80 °C for 72 h; the reaction course was controlled by TLC ($SiO_2$, eluent: dichloromethane–hexane 1 : 1 mixture). Then the reaction mixture was evaporated to dryness, the solid residue was extracted with dichloromethane (2 ml) and the extract was flash-chromatographically separated on silica gel (70 mm layer, eluent: dichloromethane–hexane 1 : 1 mixture). First two elutes were discarded; the third elute was filtered and evaporated to dryness. The solid residue was washed with ethanol and hexane, and dried *in vacuo*. Yield: 0.02 g (6%). Anal. calc. (%) for $C_{32}H_{30}B_2FeN_6O_{12}$: C, 50.04; H, 3.94; N, 10.94. Found (%): C, 50.18; H, 3.80; N, 10.90. $^1$H NMR ($CDCl_3$, $\delta$, ppm): 0.63 (t, 4H, $CH_2B$), 0.95 (t, 6H, $CH_3$), 1.42 (m, 8H, $(CH_2)_2$ (Bu)), 7.15 (m, 4H, HC(Prch)), 7.28 (m, 4H, HC(Prch)). $^{13}C\{^1H\}$ NMR ($CDCl_3$, $\delta$, ppm): 14.34 (s, $CH_3$), 26.27, 26.44 (two s, $(CH_2)_2$ (Bu)), 117.71, 125.98 (two s, HC(Prch)), 135.17 (s, OC═C), 138.67 (s, C═N). MS (MALDI-TOF): *m*/*z*: 768 $[M]^+$. UV-vis ($CH_2Cl_2$): $\lambda_{max}$, nm ($\varepsilon \times 10^{-3}$, $mol^{-1}$ L $cm^{-1}$): 268 (7.2), 282 (12), 294 (1.1), 429 (4.4), 432 (3.5), 464 (6.0), 466 (6.9).

**Fe(Cl$_2$Gm)$_2$(PrchGm)(B*n*-C$_4$H$_9$)$_2$ (6).** The complex **Fe(Cl$_2$Gm)$_3$(B*n*-C$_4$H$_9$)$_2$** (0.20 g, 0.30 mmol) was dissolved in dichloromethane (4 ml) under argon and a solution of triethylamine (0.12 ml, 0.88 mmol) and pyrocatechol (0.087 g, 0.79 mmol) in dichloromethane (2 ml) was added dropwise for 2 h to the stirring reaction mixture at −50 °C. The reaction mixture was stirred at the same temperature for 6 h; the reaction course was controlled by TLC ($SiO_2$, eluent: dichloromethane–hexane 1 : 1 mixture). Then the reaction mixture was evaporated to dryness, the solid residue was extracted with dichloromethane (2 ml) and flash-chromatographically separated on silica gel (70 mm layer, eluent: dichloromethane–hexane 1 : 1 mixture). The first orange elute was filtered and evaporated to dryness. The solid residue was washed with hexane and dried *in vacuo*. Yield: 0.145 g (69%). Anal. calc. (%) for $C_{20}H_{22}B_2Cl_4FeN_6O_8$: C, 34.63; H, 3.20; N, 12.12. Found (%): C, 34.48; H, 3.15; N, 12.17. $^1$H NMR ($CD_2Cl_2$, $\delta$, ppm): 0.66 (t, 4H, $CH_2B$), 0.97 (t, 6H, $CH_3$), 1.43 (m, 8H, $(CH_2)_2$), 7.27 (m, 2H, HC(Prch)), 7.35 (m, 2H, HC(Prch)). $^{13}C\{^1H\}$ NMR ($CD_2Cl_2$, $\delta$, ppm): 14.49 (s, $CH_3$), 16.93 (br. s, $CH_2B$), 26.36, 26.58 (two s, $(CH_2)_2$), 118.09, 126.97 (two s, HC(Prch)), 130.00 (s, ClC═N), 136.40 (s, OC═C), 138.63 (s, OC═N). MS (MALDI-TOF): *m*/*z*: 694 $[M]^+$. UV-vis ($CH_2Cl_2$): $\lambda_{max}$, nm ($\varepsilon \times 10^{-3}$, $mol^{-1}$ L $cm^{-1}$): 239 (13), 273 (13), 283 (1.0), 343 (1.5), 422 (0.9), 436 (5.4), 450 (9.8).

**Fe(Cl$_2$Gm)(PrchGm)$_2$(B*n*-C$_4$H$_9$)$_2$ (7).** The complex **Fe(Cl$_2$Gm)$_3$(B*n*-C$_4$H$_9$)$_2$** (0.30 g, 0.46 mmol) and pyrocatechol (0.31 g, 2.8 mmol) were dissolved in carbon tetrachloride (4 ml) under argon and triethylamine (0.46 ml, 3.3 mmol) was added. The reaction mixture was stirred at 75 °C for 24 h; the reaction course was controlled by TLC ($SiO_2$, eluent: dichloromethane–hexane 1 : 1 mixture). Then the reaction mixture was evaporated to dryness, the solid residue was extracted with dichloromethane (2 ml) and the extract was flash-chromatographically separated on silica gel (70 mm layer, eluent: dichloromethane–hexane 2 : 3 mixture). The first elute was discarded; the second elute was filtered and evaporated to dryness. The solid residue was washed with ethanol and hexane, and dried *in vacuo*. Yield: 0.28 g (61%). Anal. calc. (%) for $C_{26}H_{26}B_2Cl_2FeN_6O_{10}$: C, 42.73; H, 3.59; N, 11.50. Found (%): C, 42.83; H, 3.64; N, 11.60. $^1$H NMR ($CDCl_3$, $\delta$, ppm): 0.66 (t, 4H, $CH_2B$), 0.94 (t, 6H, $CH_3$), 1.42 (m, 8H, $(CH_2)_2$), 7.18 (m, 4H, HC(Prch)), 7.28 (m, 4H, HC(Prch)). $^{13}C\{^1H\}$ NMR ($CDCl_3$, $\delta$, ppm): 14.32 (s, $CH_3$), 16.81 (br. s, $CH_2B$), 26.08, 26.29 (two s, $(CH_2)_2$), 117.71, 126.22 (two s, HC(Prch)), 128.56 (s, ClC═N), 135.51 (s, OC═C), 138.41 (s, OC═N). MS (MALDI-TOF): *m*/*z*: 731 $[M]^+$. UV-vis ($CH_2Cl_2$): $\lambda_{max}$, nm ($\varepsilon \times 10^{-3}$, $mol^{-1}$ L $cm^{-1}$): 253 (5.4), 273 (13), 302 (3.7), 423 (3.3), 447 (9.6), 461 (6.5).

## X-ray crystallography

Single crystals of the complexes **Fe(Cl$_2$Gm)$_2$(*N*$_2$-Nx)(B*n*-C$_4$H$_9$)$_2$**, **Fe(PrchGm)$_3$(B*n*-C$_4$H$_9$)$_2$** and 1.5**Fe(*S*$_2$-Nx)$_2$(Cl$_2$Gm)(B*n*-C$_4$H$_9$)$_2$**·0.5**Fe(*S*$_2$-Nx)$_3$(B*n*-C$_4$H$_9$)$_2$** were grown at room temperature from dichloromethane–hexane mixtures. In the latter case, a mixture of the clathrochelate products was used for crystallization. The intensities of reflections were measured with a Bruker Apex II CCD diffractometer with multilayer optics using Cu-Kα radiation ($\lambda$ = 1.54178 Å) for the crystals 1.5**Fe(*S*$_2$-Nx)$_2$(Cl$_2$Gm)(B*n*-C$_4$H$_9$)$_2$**·0.5**Fe(*S*$_2$-Nx)$_3$(B*n*-C$_4$H$_9$)$_2$** and **Fe(PrchGm)$_3$(B*n*-C$_4$H$_9$)$_2$** and Mo-Kα radiation ($\lambda$ = 0.71073 Å, graphite monochromator) for the complex **Fe(Cl$_2$Gm)$_2$(*N*$_2$-Nx)(B*n*-C$_4$H$_9$)$_2$**. The structures were solved using the direct method and refined by full-matrix least squares against $F^2$. Non-hydrogen atoms were refined in anisotropic approximation except the disordered sulfur and chlorine atoms in the crystal 1.5**Fe(*S*$_2$-Nx)$_2$(Cl$_2$Gm)(B*n*-C$_4$H$_9$)$_2$**·0.5**Fe(*S*$_2$-Nx)$_3$(B*n*-C$_4$H$_9$)$_2$**. The asymmetric unit of the crystal 1.5**Fe(*S*$_2$-Nx)$_2$(Cl$_2$Gm)(B*n*-C$_4$H$_9$)$_2$**·0.5**Fe(*S*$_2$-Nx)$_3$(B*n*-C$_4$H$_9$)$_2$** contains two independent clathrochelate molecules. One of them is the molecule **Fe(*S*$_2$-Nx)$_2$(Cl$_2$Gm)(B*n*-C$_4$H$_9$)$_2$**, while a substantial residual density near the ribbed chlorine atoms was observed for the second macrobicyclic entity. These two peaks with high electron density values were refined as carbon atoms with partial occupancies. Free refinement of their occupancies gave values equal to 0.5; thus, an occupation of carbon atoms was fixed at 0.5. The positions of these ribbed substituents were split onto sulfur and chlorine atoms, and the S–C distances for this chelate fragment were constrained to be 1.75 Å. As a result, the second crystallographic position was found to be equiprobably occupied by the molecules **Fe(*S*$_2$-Nx)$_2$(Cl$_2$Gm)(B*n*-C$_4$H$_9$)$_2$** and **Fe(*S*$_2$-Nx)$_3$(B*n*-C$_4$H$_9$)$_2$**. The best available single crystal of the clathrochelate **Fe(Cl$_2$Gm)$_2$(*N*$_2$-Nx)(B*n*-C$_4$H$_9$)$_2$** had very poor quality that resulted in high convergence factors for its X-ray structure. H(C) atoms were included in the refinement by the riding model with $U_{iso}(H) = nU_{eq}(C)$, where $n$ = 1.5 for the methyl groups and 1.2 for the other atoms. All calculations were performed using the SHELXL[35] and OLEX2[36] program packages. The crystallographic data and experimental details are collected

in Table S1 {see the ESI†}. CCDC 1433324–1433326 contain the supplementary crystallographic data for this paper.†

## Results and discussion

Feasible pathways for the synthesis of monoribbed-functionalized iron(II) clathrochelates with apical functionalizing substituents include (i) the direct template condensation using a mixture of the corresponding α-dioximes; (ii) the condensation of a suitable macrocyclic precursor with the corresponding α-dioxime; (iii) the halogenation of a suitable glyoximate clathrochelate precursor; and (iv) the partial and stepwise nucleophilic substitution of the apically functionalized metal hexachloroclathrochelates. It should be noted that the dihalogeno-α-dioximate ligands are substantially weaker donors than their aliphatic and aromatic analogs. As a result, the use of a mixture of the corresponding α-dioximes in the direct template condensation leads mainly to $C_3$-symmetric clathrochelate products with equivalent ribbed fragments, but not the target cage complexes with non-equivalent chelate moieties. Condensation of macrocyclic bis-α-dioximates with these weakly donor dihalogenodioximes typically proceeds under vigorous reaction conditions, also giving $C_3$-symmetric boron-capped aliphatic or aromatic tris-dioximates as the clathrochelate products of a symmetrization reaction. Moreover, the preparation of the above macrocyclic bis-dioximates, the derivatives of the corresponding functionalized boronic acids, as their precursors, seems to be a real synthetic challenge. Halogenation of apically functionalized glyoximate macrobicyclic complexes is complicated by side reactions of their apical and ribbed substituents, as well as by the complete destruction of their cage frameworks under these reaction conditions. Therefore, the latter pathway (iv) seems to be the most convenient: metal(II) hexahalogenoclathrochelates can be obtained in high yields using the direct template condensation on the metal(II) ion as a matrix.[13,17,18] Their nucleophilic substitution with several bis-nucleophiles, forming stable six-membered alicyclic ribbed fragments,[37,38] can be performed stepwise, thus giving the corresponding di- and tetrahalogenoclathrochelate precursors. Moreover, it was shown[39] that nucleophilic substitution of *vic*-dichloroclathrochelates with secondary aliphatic amines as *N*-nucleophiles gives the monoamine macrobicyclic products of such substitution of only one of the two chlorine atoms in the *vic*-position of the same ribbed fragment. This partial functionalization allows obtaining the corresponding monohalogenoclathrochelates, which can undergo further nucleophilic substitution with more active nucleophiles, such as primary aliphatic amines and thiolate anions.

Analogous synthetic pathways can also be used for the synthesis of tetrahalogenoclathrochelates. In this case, the preparation of their macrocyclic tetrahalogeno-bis-α-dioximate precursors seems to be especially questionable. Stepwise nucleophilic substitution using different bis-nucleophilic agents allows obtaining dichloroclathrochelate complexes with non-equivalent alicyclic ribbed substituents, such as $N_2$- and $S_2$-containing six-membered cycles. It should be noted that the remaining halogen atoms of the tetraamine iron(II) dihalogenoclathrochelates are unreactive under standard conditions of this reaction.[39] In general, the inherent electron-donating amine groups at a quasiaromatic polyazomethine cage framework deactivate the remaining halogen substituents and, as a result, they do not undergo nucleophilic substitution even at high temperatures and with a large excess of a nucleophilic agent as well. In the case of anionic forms of ethylenediamine and 1,2-ethanedithiol as $N_2$- and $S_2$-bis-nucleophiles, generated *in situ* in the presence of triethylamine, such substitution proceeds easily and in a high yield due to the formation of stable six-membered alicyclic ribbed substituents at a macrobicyclic framework. Indeed, six-membered alicycles are most less strained,[40] and therefore, cyclohexane-based metal tris-dioximate clathrochelates are substantially more stable than their cycloheptane-containing analogs,[1] whereas the chelate complexes of cyclopentanedione-1,2 dioxime have not been reported in the literature to date. Previously, 1,2-ethanedithiol and ethylenediamine have been successfully used for the preparation of $N_2$- and $S_2$-alicyclic mono- and triribbed-functionalized iron, ruthenium(II), and cobalt(II,III) clathrochelates.[37,38] They have been prepared in relatively high yields using intramolecular nucleophilic substitution (cyclization) and pseudo-high dilution reaction conditions, thus limiting the formation of various macrobicyclic by-products, which are known to be usually formed in the case of such polynucleophilic agents.

At the same time, nucleophilic substitution with anionic derivatives of aliphatic diols as $O_2$-bis-nucleophiles proceeds without the destruction of a tris-dioximate clathrochelate framework only at very low temperatures in the presence of cadmium(II) amides as promoters, giving the target $O_2$-alicyclic cage products in low yields.[22] In contrast, the same reactions with phenolate anions or pyrocatechol-based podands as *O*-nucleophiles gave di- and triribbed-functionalized macrobicyclic tetra- and hexaphenolates, and bis- and tris-crown ether iron and ruthenium(II) clathrochelates, respectively, in moderate yields.[17,18] So, we used nucleophilic substitution with anionic derivatives of pyrocathechol, generated *in situ* in the presence of triethylamine, for the preparation of iron(II) di- and tetrachloroclathrochelate precursors with $O_2$-containing six-membered cyclic ribbed substituent(s).

In the case of anionic derivatives of ethylenediamine as $N_2$-bis-nucleophiles, only mono-$N_2$-alicyclic iron(II) tetrachloroclathrochelate **Fe($N_2$-Nx)($Cl_2$Gm)$_2$(B*n*-$C_4H_9$)$_2$** was obtained in a moderate yield. We failed to isolate its bis-$N_2$-alicyclic dichloroclathrochelate analog even in a low yield: the use of an excess of ethylenediamine led to complete destruction of a cage framework. At the same time, the tetrachloroclathrochelate **Fe($S_2$-Nx)($Cl_2$Gm)$_2$(B*n*-$C_4H_9$)$_2$** undergoes further nucleophilic substitution of one of its two dichloroglyoximate fragments as shown in Scheme 2, thus giving $N_2$, $S_2$-alicyclic dichloroclathrochelate **Fe($N_2$-Nx)($S_2$-Nx)($Cl_2$Gm)$_2$(B*n*-$C_4H_9$)$_2$** with three non-equivalent ribbed chelate fragments. However, this complex cannot be regarded as a dichloroclathrochelate precursor: its two remaining chlorine atoms do not undergo nucleophilic substitution under standard reaction conditions. Their low reactivity is caused by the electron-donating effect of the inherent alicyclic diamine substituent at a quasiaromatic cage framework of **Fe($N_2$-Nx)($S_2$-Nx)($Cl_2$Gm)$_2$(B*n*-$C_4H_9$)$_2$**. The same effect has been previously observed[17,18,39]

 

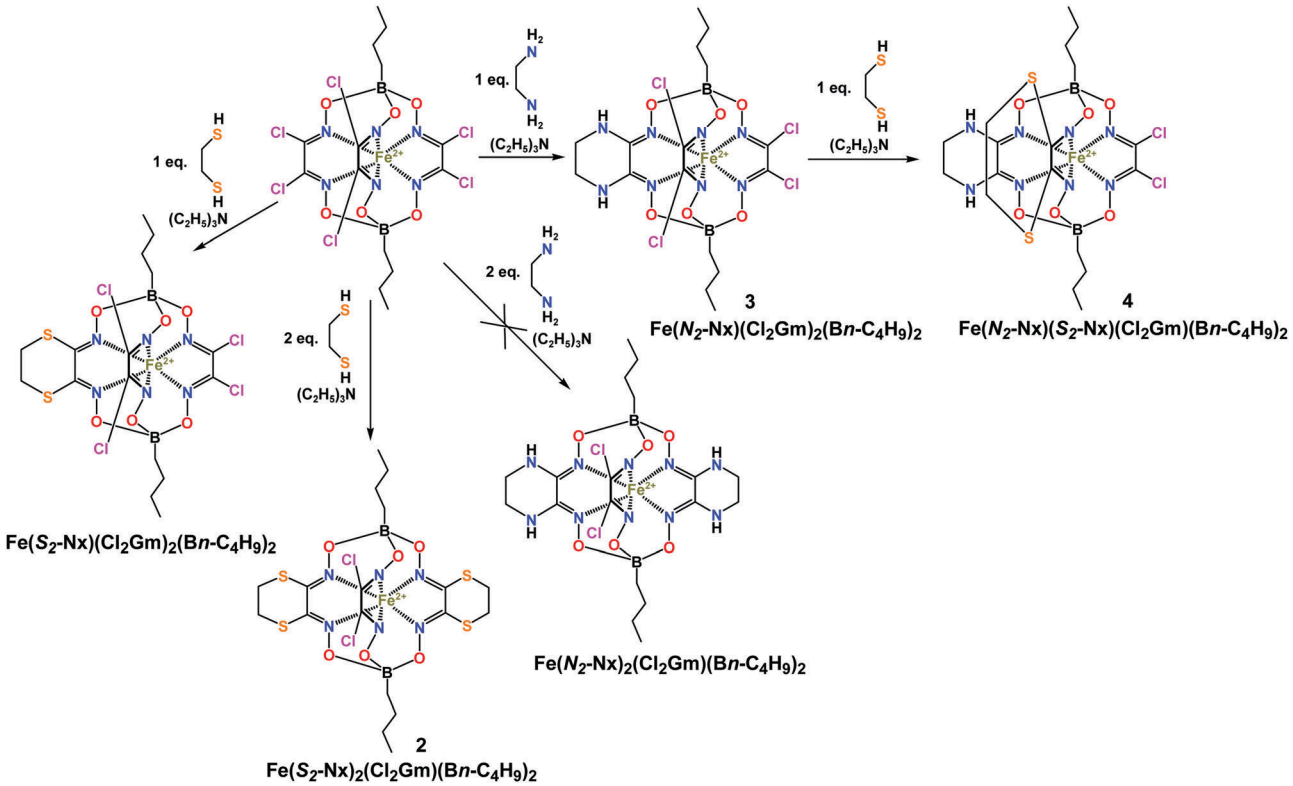


Scheme 2 Synthesis of $S_2$- and $N_2$-alicyclic di- and tetrachloroclathrochelates.

in a series of amine iron and ruthenium(II) tris-dioximate clathrochelates.

Stepwise nucleophilic substitution with anionic derivatives of 1,2-ethanedithiol allowed us to obtain both mono- and diribbed-substituted $S_2$-alicyclic tetra- and dichloroclathrochelates **Fe($S_2$-Nx)(Cl$_2$Gm)$_2$(B*n*-C$_4$H$_9$)$_2$** and **Fe($S_2$-Nx)$_2$(Cl$_2$Gm)(B*n*-C$_4$H$_9$)$_2$** (Scheme 2). These cage complexes were obtained using a classical approach of macrocyclic chemistry[41–44] under pseudo-high dilution conditions by a simultaneous dropwise addition of the reagents (*i.e.* the hexadichloroclathrochelate **Fe(Cl$_2$Gm)$_3$(B*n*-C$_4$H$_9$)$_2$** and 1,2-ethanedithiol) in their molar ratios 1 : 1 and 1 : 2, respectively, to the intensively stirring solvent. However, in both these cases, the target clathrochelates were contaminated by their triribbed-functionalized analog **Fe($S_2$-Nx)$_3$(B*n*-C$_4$H$_9$)$_2$** and these mixtures are poorly separable even by column chromatography.

We also performed the study of a stepwise nucleophilic substitution of the hexachloroclathrochelate precursor **Fe(Cl$_2$Gm)$_3$(B*n*-C$_4$H$_9$)$_2$** with the pyrocatecholate dianion. Mono- and bis-pyrocatecholate macrobicyclic products **Fe(Cl$_2$Gm)$_2$(PrchGm)(B*n*-C$_4$H$_9$)$_2$** and **Fe(Cl$_2$Gm)(PrchGm)$_2$(B*n*-C$_4$H$_9$)$_2$** were obtained in relatively high yields using clathrochelate precursor-to-nucleophile molar ratios 1 : 1 and 1 : 2, respectively (Scheme 3). At the same time, we did not detect the corresponding tris-pyrocatecholate cage complex with equivalent ribbed fragments among the clathrochelate products of nucleophilic substitution under standard conditions of this reaction. Such a $C_3$-symmetric complex was obtained in a low yield (approximately 7%) only under vigorous reaction conditions with a large excess of pyrocatechol at high temperature using a boiling nitromethane as a solvent. In contrast, aiming to obtain the monoribbed-functionalized tetrachloroclathrochelate of this type, the complex **Fe(Cl$_2$Gm)$_2$(PrchGm)(B*n*-C$_4$H$_9$)$_2$**, and trying to avoid the formation of the bis-pyrocatecholate iron(II) macrobicyclic complex, we performed nucleophilic substitution at low temperature (−50 °C) in dichloromethane medium, thus allowing an increase in its yield of up to approximately 70%. At the same time, the complex **Fe(Cl$_2$Gm)(PrchGm)$_2$(B*n*-C$_4$H$_9$)$_2$** was obtained in a relatively high yield in carbon tetrachloride as a solvent, allowing performing this reaction at approximately 75 °C.

The complexes obtained were characterized using elemental analysis, MALDI-TOF mass spectrometry, and IR, UV-vis, $^1$H and $^{13}$C{$^1$H} NMR spectroscopies, and by single crystal X-ray diffraction.

The numbers and positions of the signals in the solution $^1$H and $^{13}$C{$^1$H} NMR spectra of the diamagnetic iron(II) di- and tetrachloroclathrochelates and their derivatives (see the ESI,† Fig. S1–S16), and the ratios of the integral intensities of protons of the apical *n*-butyl groups, the aliphatic and aromatic chelate fragments and those of the functionalizing ribbed substituents in their $^1$H NMR spectra confirmed the compositions and symmetries of the macrobicyclic molecules obtained, thus allowing deducing their chemical constitution. In particular, the $^{13}$C{$^1$H} NMR spectra of monoribbed-functionalized iron(II) tetrachloroclathrochelates **Fe($N_2$-Nx)(Cl$_2$Gm)$_2$(B*n*-C$_4$H$_9$)$_2$** and **Fe($S_2$-Nx)(Cl$_2$Gm)$_2$(B*n*-C$_4$H$_9$)$_2$**, as well as those of the diribbed-functionalized dichloroclathrochelate **Fe($S_2$-Nx)$_2$(Cl$_2$Gm)(B*n*-C$_4$H$_9$)$_2$**, the derivative of 1,2-ethanedithiol, whose molecules

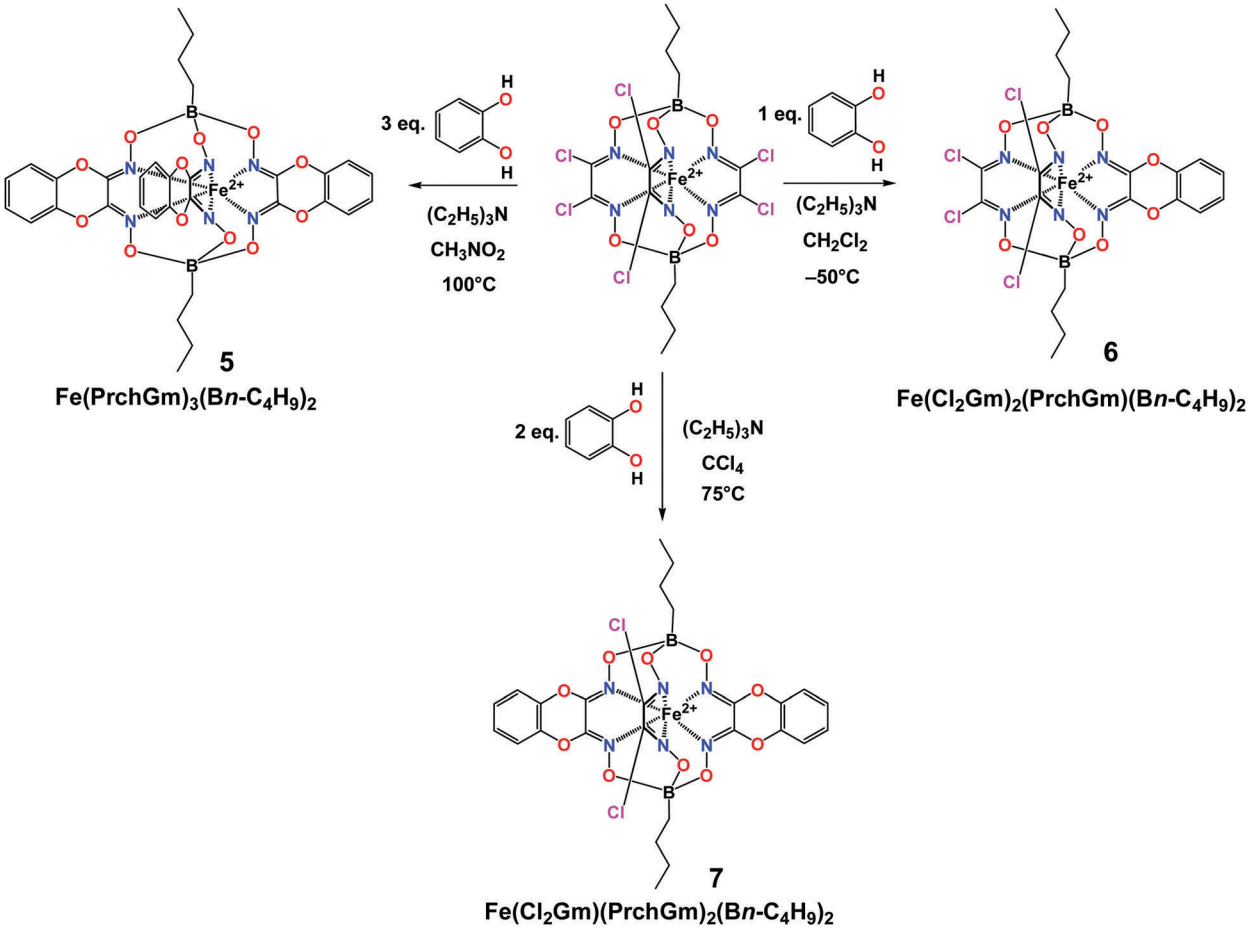


Scheme 3 Synthesis of pyrocatechol cage complexes.

have a symmetry plane passing through their B···Fe···B axes, contain the signals of azomethine carbon atoms of two types. On the other hand, that of their analog **Fe($N_2$-Nx)($S_2$-Nx)($Cl_2$Gm)-(B*n*-$C_4H_9$)$_2$** with all the non-equivalent chelate fragment contains three signals of this type in the range 120–145 ppm: its molecule does not have the molecular $C_3$ symmetry pseudoaxis, passing through the capping boron atoms, but it has a symmetry plane, passing through the middles of the chelate C–C bonds and this caged ion as well.

The molecular structures of the ribbed-functionalized iron(II) clathrochelates **Fe($Cl_2$Gm)$_2$($N_2$-Nx)(B*n*-$C_4H_9$)$_2$**, **Fe(PrchGm)$_3$(B*n*-$C_4H_9$)$_2$**, **Fe($S_2$-Nx)$_2$($Cl_2$Gm)(B*n*-$C_4H_9$)$_2$** and·**Fe($S_2$-Nx)$_3$(B*n*-$C_4H_9$)$_2$** are shown in Fig. 1–3; the main geometrical parameters of their macrobicyclic molecules are listed in Table 1. The Fe–N distances in these molecules fall within a narrow range (1.91–1.93 Å) and are characteristic of iron(II) tris-dioximate clathrochelates.[1,2] A cage framework of the iron(II) complex **Fe($Cl_2$Gm)$_2$($N_2$-Nx)(B*n*-$C_4H_9$)$_2$** is similar to those of the amine clathrochelates **Fe(($C_6H_{11}NH$)$_2$Gm)$_2$-($Cl_2$Gm)($BC_6H_5$)$_2$**[39] and **Fe((*n*-$C_4H_9NH$)$_2$Gm)$_2$($Cl_2$Gm)($BC_6H_5$)$_2$** with non-equivalent ribbed fragments.[17] The encapsulated iron(II) ion is slightly shifted from the geometrical centers of their macrobicyclic frameworks in the direction of the α-dichloroglyoximate chelate fragment. The C–C bond lengths in these fragments (1.41–1.45 Å) are shorter than those in the amine chelate ribbed fragment (1.47 Å).

The Fe–N distances in the di- and triribbed-functionalized macrobicyclic molecules of the crystal 1.5**Fe($S_2$-Nx)$_2$($Cl_2$Gm)(B*n*-$C_4H_9$)$_2$**·0.5**Fe($S_2$-Nx)$_3$(B*n*-$C_4H_9$)$_2$** vary from 1.903(3) to 1.912(4) Å, thus being slightly smaller than those for their tris-pyrocatecholate clathrochelate analog (1.928(1)–1.935(1) Å). Although in all the cases the geometry of their $FeN_6$-coordination polyhedra is intermediate between a trigonal prism (TP, the distortion angle $\varphi = 0^\circ$) and a trigonal antiprism (TAP, $\varphi = 60^\circ$), passing to the molecule **Fe(PrchGm)$_3$(B*n*-$C_4H_9$)$_2$** is accompanied by elongation of the Fe–N bonds and by an increase in $\varphi$ from 23.4 to 26.5° due to a rotational–translational elongation of its cage framework. The height $h$ of the corresponding coordination polyhedron is slightly greater (2.41 Å) as compared to those in the range 2.34–2.36 Å which have been observed for its *n*-butylboron-capped tetra- and hexafunctionalized clathrochelate analogs.[1,2] Other geometrical parameters of their macrobicyclic frameworks are also characteristic of the boron-capped clathrochelate iron(II) tris-dioximates.

Strong intermolecular bonding is observed only in the crystal **Fe($Cl_2$Gm)$_2$($N_2$-Nx)(B*n*-$C_4H_9$)$_2$** that contains the intermolecular N–H···O connected chains with a distance of $r_i$(N···O) = 3.309(8) Å and with an N···H···O angle of approximately 157°, which are parallel to its crystallographic axis *b* (Fig. 4). In contrast, only weak intermolecular C–H···π and C–H···O interactions are observed in the crystals 1.5**Fe($S_2$-Nx)$_2$($Cl_2$Gm)(B*n*-$C_4H_9$)$_2$**·0.5**Fe($S_2$-Nx)$_3$(B*n*-$C_4H_9$)$_2$**

 

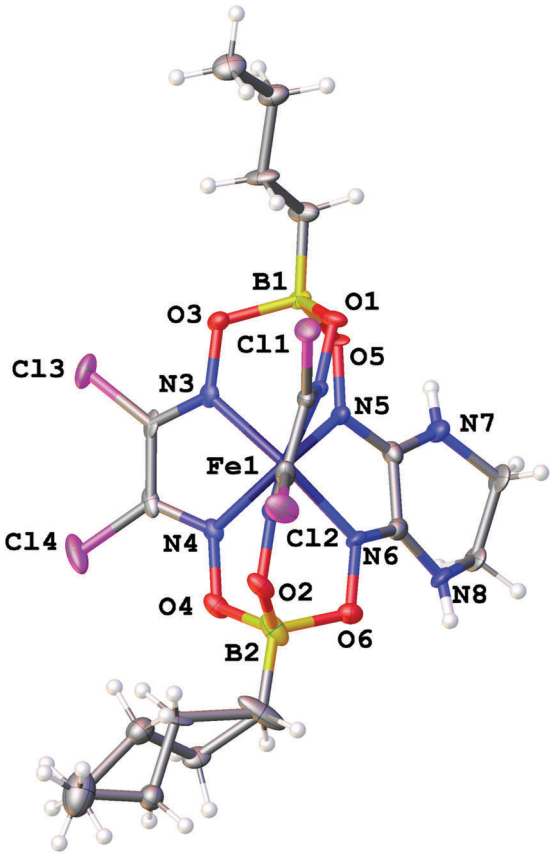


Fig. 1 General view of the molecule **Fe(Cl$_2$Gm)$_2$($N_2$-Nx)(B*n*-C$_4$H$_9$)$_2$** in representation of atoms with thermal ellipsoids given with $p$ = 50%. One of its apical *n*-butyl substituents is equiprobably disordered over two sites.

and **Fe(PrchGm)$_3$(B*n*-C$_4$H$_9$)$_2$**. The absence of strong intermolecular bonding in the case of the clathrochelates **Fe($S_2$-Nx)$_2$(Cl$_2$Gm)(B*n*-C$_4$H$_9$)$_2$** and **Fe($S_2$-Nx)$_3$(B*n*-C$_4$H$_9$)$_2$** resulted in their co-crystallization, thus giving the corresponding co-crystals.

Similar co-crystallization of the different clathrochelates has been previously observed[15] for the two constitutional isomers of the complex **Fe(CH$_3$ClGm)(CH$_3$(*n*-C$_4$H$_9$NH)Gm)$_2$(BC$_6$H$_5$)$_2$**: 10% impurity of the chloroform solvate of its *mer*,*fac*,*fac*-isomer in the crystal of a *mer*,*mer*-isomer of this complex was detected. The co-crystal **FeBd$_2$((CF$_3$)$_2$Gm)(BF)$_2$·FeBd$_2$((CF$_3$)GmI)(BF)$_2$·2C$_6$H$_{14}$** that is isostructural to the complex **FeBd$_2$((CF$_3$)$_2$Gm)(BF)$_2$·C$_6$H$_{14}$** is described;[45] it should be noted that the attempted crystallization of a pure clathrochelate **FeBd$_2$((CF$_3$)GmI)(BF)$_2$** met with failure.[45]

Deconvolution of UV-vis spectra of the $O_2$-, $S_2$-, $N_2$- and $N_2$,$S_2$-alicyclic iron(II) di- and tetrachloroclathrochelates under study (see the ESI,† Fig. S17–S23) into their Gaussian components gave in the visible range from two to six intense metal-to-ligand charge transfer (MLCT) Fe$d$ → L$\pi^*$ bands, respectively, with maxima in the range 410–600 nm; the bands of $\pi$–$\pi^*$ transitions in their polyazomethine macrobicyclic ligands were observed in the range 240–380 nm (see the ESI,† Table S2). The spectrum of the hexachloroclathrochelate **Fe(Cl$_2$Gm)$_3$(B*n*-C$_4$H$_9$)$_2$** in its visible range contains two MLCT bands with maxima at approximately 420 and 450 nm. Thus, passing from two chlorine atoms in this dichloroclathrohelate molecule to its derivatives with $O_2$-, $S_2$-, $N_2$- and $N_2$, $S_2$-alicyclic ribbed fragments led to a substantial (up to 40 nm) shift of the longwave band of this type and to the appearance of up to four new bands with maxima in the range 580–600 nm. This fact is indicative of a dramatic redistribution of the electron density in a quasiaromatic clathrochelate framework caused by its ribbed functionalization with six-membered $O_2$-, $S_2$- and $N_2$-alicyclic substituent(s).

Table 1 Main geometrical parameters of the iron(II) clathrochelates with $N_2$-, $S_2$- and $O_2$-alicyclic ribbed substituents

| | | **Fe($S_2$-Nx)$_2$(Cl$_2$Gm)(B$_n$-C$_4$H$_9$)$_2$** | | |
|---|---|---|---|---|
| Parameter | **Fe(Cl$_2$Gm)$_2$($N_2$-Nx)(B*n*-C$_4$H$_9$)$_2$** | Type A | Type B | **Fe(PrchGm)$_3$(B*n*-C$_4$H$_9$)$_2$**[b] |
| Fe–N(1) (Å) | 1.905(6) | 1.912(4)[a] | 1.909(4)[a] | 1.928(1) |
| Fe–N(2) (Å) | 1.918(6) | 1.904(4)[a] | 1.906(3)[a] | 1.935(1) |
| Fe–N(3) (Å) | 1.914(6) | 1.905(4) | 1.911(3) | 1.928(1) |
| Fe–N(4) (Å) | 1.913(6) | 1.910(4) | 1.903(3) | |
| Fe–N(5) (Å) | 1.933(6)[a] | 1.909(4) | 1.903(3) | |
| Fe–N(6) (Å) | 1.934(6)[a] | 1.906(4) | 1.907(4) | |
| B–O (Å) | 1.497(10)–1.538(11) | 1.499(6)–1.512(6) | 1.495(6)–1.524(5) | 1.505(2)–1.517(2) |
| | *av.* 1.519 | *av.* 1.506 | *av.* 1.509 | *av.* 1.510 |
| N–O (Å) | 1.353(8)–1.415(7) | 1.364(5)–1.382(5) | 1.355(4)–1.373(4) | 1.369(1)–1.376(1) |
| | *av.* 1.379 | *av.* 1.372 | *av.* 1.366 | *av.* 1.374 |
| C=N (Å) | 1.283(9)–1.325(9) | 1.293(6)–1.313(5) | 1.300(5)–1.317(5) | 1.291(2)–1.300(2) |
| | *av.* 1.308 | *av.* 1.303 | *av.* 1.307 | *av.* 1.295 |
| C–C (Å) | 1.417(11)–1.469(10) | 1.430(7)–1.449(6) | 1.429(6)–1.449(6) | 1.438(3)–1.444(2) |
| | *av.* 1.443 | *av.* 1.439 | *av.* 1.440 | *av.* 1.442 |
| B–C (Å) | 1.570(11)–1.580(11) | 1.575(7)–1.587(7) | 1.570(6)–1.576(6) | 1.594(2) |
| | *av.* 1.575 | *av.* 1.365 | *av.* 1.573 | |
| N=C–C=N (°) | 9.0(11)–10.5(7) | 7.8(6)–10.8(7) | 4.1(5)–10.7(4) | 8.5(2)–9.2(2) |
| | *av.* 10.0 | *av.* 9.3 | *av.* 8.5 | *av.* 9.0 |
| $\varphi$ (°) | 26.5 | 25.3 | 24.0 | 23.4 |
| $\alpha$ (°) | 79.6 | 79.4 | 79.0 | 80.0 |
| $h$ (Å) | 2.36 | 2.34 | 2.34 | 2.41 |

[a] The distance for the functionalized ribbed fragment. [b] Only half of this molecule is symmetrically independent.

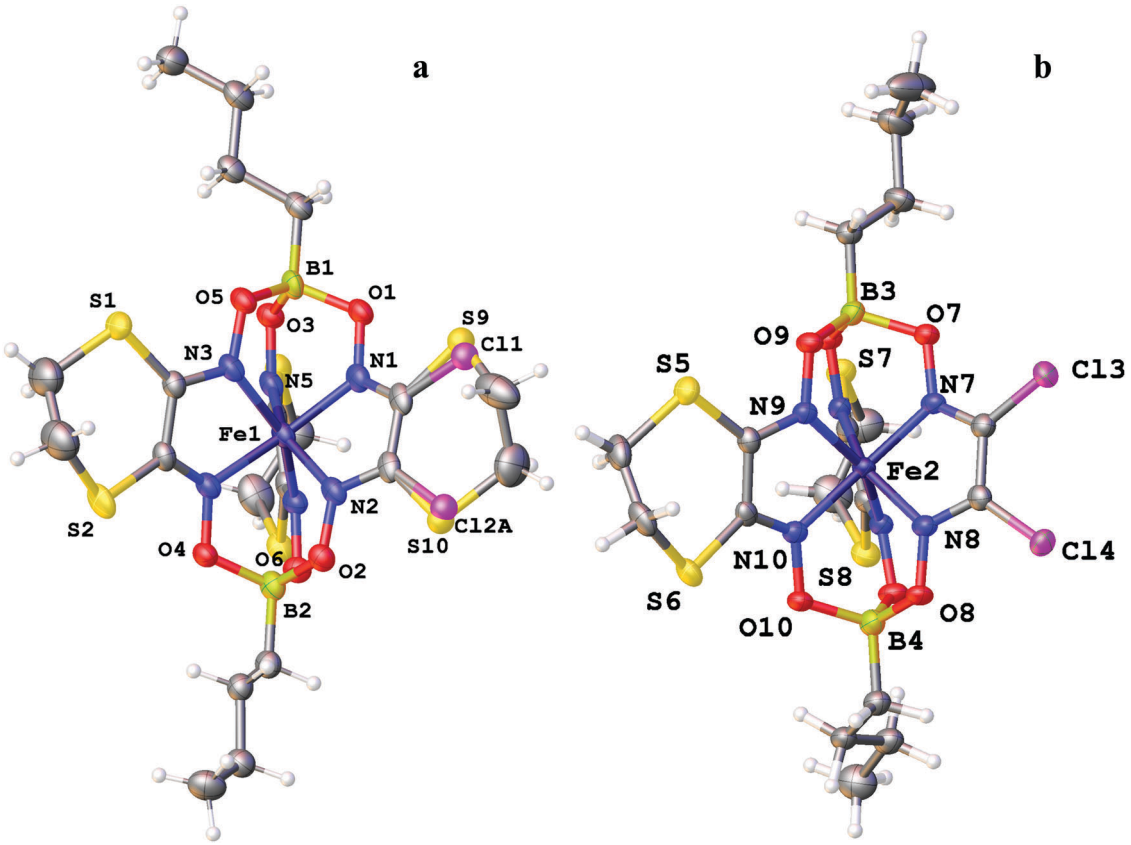


Fig. 2 General views of the disordered (a) and ordered (b) molecules of the clathrochelate **Fe($S_2$-Nx)$_2$($Cl_2$Gm)(B*n*-$C_4H_9$)$_2$** in representation of atoms with thermal ellipsoids given with $p$ = 50%. The disordered crystallographic site is equiprobably occupied by the macrobicycles **Fe($S_2$-Nx)$_3$(B*n*-$C_4H_9$)$_2$** and **Fe($S_2$-Nx)$_2$($Cl_2$Gm)(B*n*-$C_4H_9$)$_2$**.

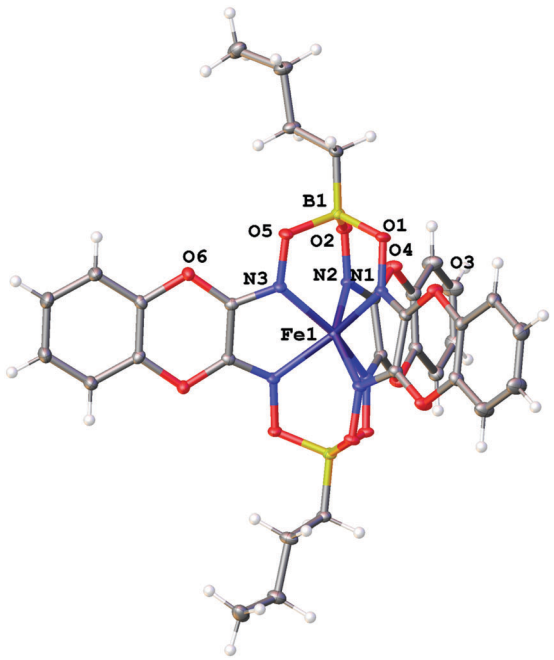


Fig. 3 General view of the clathrochelate **Fe(PrchGm)$_3$(B*n*-$C_4H_9$)$_2$** in representation of atoms with thermal ellipsoids given with $p$ = 50%. Only half of its molecule is symmetrically independent.

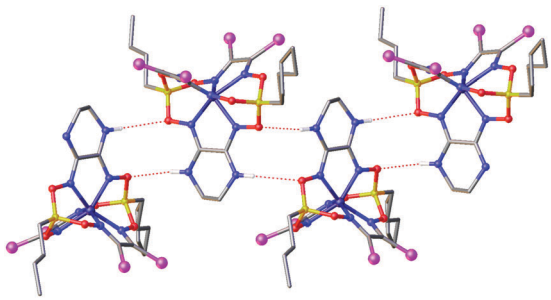

Fig. 4 Hydrogen bonding between the clathrochelate molecules in the crystal **Fe($Cl_2$Gm)$_2$($N_2$-Nx)(B*n*-$C_4H_9$)$_2$**. Hydrogen atoms, which do not form such supramolecular bonds, are omitted for clarity.

## Conclusion

Thus, we developed straightforward synthetic strategies and convenient procedures allowing a gram-scale synthesis of various types of di- and tetrachloroclathrochelates, which seem to be suitable macrobicyclic precursors for the preparation of a wide range of cage complexes of given symmetry and functionality for their further biological testing in different *in vitro*, *ex vivo* and *in vivo* systems.

 

## Conflicts of interest

There are no conflicts to declare.

## Acknowledgements

The synthesis of cage complexes was supported by the Russian Science Foundation (grant 16-13-10475). The spectral and X-ray diffraction studies were performed with the financial support of the EU Research and Innovation Staff Exchange (RISE) (H2020-MSCA-RISE-2017, Project 778245 'CLATHROPROBES'). The contribution of the Center for molecule composition studies of INEOS RAS is gratefully acknowledged. A. S. B., G. E. Z. and I. G. B. also thank the RFBR (grants 17-03-00587, 16-33-00146 and 16-33-60196) for the financial support.

## References

1 Y. Z. Voloshin, N. A. Kostromina and R. Krämer, *Clathrochelates: Synthesis, Structure and Properties*, Elsevier, Amsterdam, 2002.
2 Y. Z. Voloshin, I. G. Belaya and R. Krämer, *Cage metal complexes: clathrochelates revisited*, Springer, Heidelberg, 2017.
3 Y. Z. Voloshin, V. V. Novikov and Y. V. Nelyubina, *RSC Adv.*, 2015, **5**, 72621–72637.
4 V. V. Novikov, O. A. Varzatskii, V. V. Negrutska, Y. N. Bubnov, L. G. Palchykovska, I. Y. Dubey and Y. Z. Voloshin, *J. Inorg. Biochem.*, 2013, **124**, 42–45.
5 A. S. Belov, A. V. Vologzhanina, V. V. Novikov, V. V. Negrutska, I. Y. Dubey, Z. A. Mikhailova, E. G. Lebed and Y. Z. Voloshin, *Inorg. Chim. Acta*, 2014, **421**, 300–306.
6 O. A. Varzatskii, V. V. Novikov, S. V. Shulga, A. S. Belov, A. V. Vologzhanina, V. V. Negrutska, I. Y. Dubey, Y. N. Bubnov and Y. Z. Voloshin, *Chem. Commun.*, 2014, **50**, 3166–3168.
7 A. Oleksy, A. G. Blanco, R. Boer, I. Uson, J. Aymami, A. Rodger, M. J. Hannon and M. Coll, *Angew. Chem., Int. Ed.*, 2006, **45**, 1227–1231.
8 Y. Z. Voloshin, K. Y. Zhizhin, V. V. Novikov, O. A. Varzatskii and N. T. Kuznetsov, 16th International Seminar on Inclusion Compounds (ISIC-16), Kazan (Russia), June 26–30, 2017, p. 36.
9 M. Y. Losytskyy, V. B. Kovalska, O. A. Varzatskii, A. M. Sergeev, S. M. Yarmoluk and Y. Z. Voloshin, *J. Fluoresc.*, 2013, **23**, 889–895.
10 V. B. Kovalska, M. Y. Losytskyy, O. A. Varzatskii, V. V. Cherepanov, Y. Z. Voloshin, A. A. Mokhir, S. M. Yarmoluk and S. V. Volkov, *Bioorg. Med. Chem.*, 2014, **22**, 1883–1888.
11 J. Blechinger, O. A. Varzackii, V. Kovalska, G. E. Zelinskii, Y. Z. Voloshin, E. Kinski and A. Mokhir, *Bioorg. Med. Chem. Lett.*, 2016, **26**, 626–629.
12 Y. Z. Voloshin, V. E. Zavodnik, O. A. Varzatskii, V. K. Belsky, A. V. Palchik, N. G. Strizhakova and M. Y. Antipin, *Dalton Trans.*, 2002, 1193.
13 Y. Z. Voloshin, O. A. Varzatskii, V. V. Novikov, N. G. Strizhakova, I. I. Vorontsov, A. V. Vologzhanina, K. A. Lyssenko, G. V. Romanenko, M. V. Fedin, V. I. Ovcharenko and Y. N. Bubnov, *Eur. J. Inorg. Chem.*, 2010, 5401–5415.
14 Y. Z. Voloshin, O. A. Varzatskii, A. V. Palchik, Z. A. Starikova, M. Yu. Antipin, E. G. Lebed and Y. N. Bubnov, *Inorg. Chim. Acta*, 2006, **359**, 553–569.
15 Y. Z. Voloshin, O. A. Varzatskii, A. V. Palchik, I. I. Vorontsov, M. Y. Antipin and E. G. Lebed, *Inorg. Chim. Acta*, 2005, **358**, 131–146.
16 Y. Z. Voloshin, A. S. Belov, A. V. Vologzhanina, G. G. Aleksandrov, A. V. Dolganov, V. V. Novikov, O. A. Varzatskii and Y. N. Bubnov, *Dalton Trans.*, 2012, **41**, 6078–6093.
17 Y. Z. Voloshin, O. A. Varzatskii, T. E. Kron, V. K. Belsky, V. E. Zavodnik, N. G. Strizhakova and A. V. Palchik, *Inorg. Chem.*, 2000, **39**, 1907–1918.
18 Y. Z. Voloshin, O. A. Varzatskii, T. E. Kron, V. K. Belsky, V. E. Zavodnik, N. G. Strizhakova, V. A. Nadtochenko and V. A. Smirnov, *Dalton Trans.*, 2002, 1203–1211.
19 O. I. Artyushin, I. L. Odinets, E. V. Matveeva, A. V. Vologzhanina, O. A. Varzatskii, S. E. Lubimov and Y. Z. Voloshin, *Dalton Trans.*, 2014, **43**, 9677–9689.
20 O. I. Artyushin, E. V. Matveeva, A. V. Vologzhanina and Y. Z. Voloshin, *Dalton Trans.*, 2016, **45**, 5328–5333.
21 Y. Z. Voloshin, O. A. Varzatskii, P. A. Stuzhin, S. V. Shul'ga, S. V. Volkov, A. V. Vologzhanina, E. G. Lebed and Y. N. Bubnov, *Inorg. Chem. Commun.*, 2011, **14**, 1504–1507.
22 O. A. Varzatskii, Y. Z. Voloshin, S. V. Korobko, S. V. Shulga, R. Krämer, A. S. Belov, A. V. Vologzhanina and Y. N. Bubnov, *Polyhedron*, 2009, **28**, 3431–3438.
23 M. A. Vershinin, A. B. Burdukov, I. V. Eltsov, V. A. Reznikov, E. G. Boguslavsky and Y. Z. Voloshin, *Polyhedron*, 2011, **30**, 1233–1237.
24 A. B. Burdukov, M. A. Vershinin, N. V. Pervukhina, S. G. Kozlova, I. V. Eltsov and Y. Z. Voloshin, *Russ. Chem. Bull.*, 2011, **60**, 2504–2509.
25 M. A. Vershinin, A. B. Burdukov, N. V. Pervukhina, I. V. Eltsov and Y. Z. Voloshin, *Macroheterocycles*, 2012, **5**, 11–16.
26 M. A. Vershinin, A. B. Burdukov, N. V. Pervukhina, I. V. Eltsov and Y. Z. Voloshin, *Macroheterocycles*, 2015, **8**, 71–74.
27 M. A. Vershinin, A. B. Burdukov, N. V. Pervukhina, I. V. Eltsov and Y. Z. Voloshin, *Inorg. Chem. Commun.*, 2013, **30**, 159–162.
28 M. A. Vershinin, A. B. Burdukov, N. V. Pervukhina and I. V. Eltsov, *J. Struct. Chem.*, 2015, **56**, 379–381.
29 Y. Z. Voloshin, A. S. Belov, O. A. Varzatskii, S. V. Shul'ga, P. A. Stuzhin, Z. A. Starikova, E. G. Lebed and Y. N. Bubnov, *Dalton Trans.*, 2012, **41**, 921–928.
30 M. A. Vershinin, A. B. Burdukov, E. G. Boguslavskii, N. V. Pervukhina, N. V. Kuratieva, I. V. Eltsov, V. A. Reznikov, O. A. Varzatskii, Y. Z. Voloshin and Y. N. Bubnov, *Inorg. Chim. Acta*, 2011, **366**, 91–97.
31 A. B. Burdukov, R. Šipoš, M. A. Vershinin, N. V. Pervukhina, N. V. Kuratieva, P. E. Plyusnin, I. V. Eltsov and Y. Z. Voloshin, *J. Coord. Chem.*, 2015, **68**, 3894–3902.
32 Y. Z. Voloshin, O. A. Varzatskii, S. V. Shul'ga, I. N. Denisenko, A. V. Vologzhanina and Y. N. Bubnov, *Inorg. Chem. Commun.*, 2012, **17**, 128–131.
33 O. A. Varzatskii, S. V. Shul'ga, A. S. Belov, V. V. Novikov, A. V. Dolganov, A. V. Vologzhanina and Y. Z. Voloshin, *Dalton Trans.*, 2014, **43**, 17934–17948.
34 M. Wojdyr, *J. Appl. Crystallogr.*, 2010, **43**, 1126–1128.

35 G. M. Sheldrick, *Acta Crystallogr., Sect. C: Struct. Chem.*, 2015, **71**, 3–8.
36 O. V. Dolomanov, L. J. Bourhis, R. J. Gildea, J. A. K. Howard and H. Puschmann, *J. Appl. Crystallogr.*, 2009, **42**, 339–341.
37 Y. Z. Voloshin, O. A. Varzatskii, A. S. Belov, Z. A. Starikova, N. G. Strizhakova, A. V. Dolganov, D. I. Kochubey and Y. N. Bubnov, *Inorg. Chim. Acta*, 2010, **363**, 134–146.
38 Y. Z. Voloshin, O. A. Varzatskii, A. S. Belov, Z. A. Starikova, A. V. Dolganov, V. V. Novikov and Y. N. Bubnov, *Inorg. Chim. Acta*, 2011, **370**, 322–332.
39 V. E. Zavodnik, O. A. Varzatskii, V. K. Belsky, I. I. Vorontsov and M. Y. Antipin, *Inorg. Chim. Acta*, 2001, **321**, 116–134.
40 D. Barton and W. D. Ollis, *Comprehensive organic chemistry*, Pergamon, Oxford, 1979.
41 R. M. Izatt and J. J. Christensen, *Synthesis of macrocycles, The design of selective complexing agents*, Wiley-Interscience, New York, 1987.
42 D. Parker, *Macrocycle synthesis: a practical approach*, Oxford University Press, Oxford, 1996.
43 N. V. Gerbeleu, V. B. Arion and F. J. Burgess, *Template synthesis of macrocyclic compounds*, Wiley-VCH, Weinheim, 2000.
44 F. Diederich, P. J. Stang and R. R. Tykwinski, *Modern supramolecular chemistry: strategies for macrocycle synthesis*, Wiley-VCH, Weinheim, 2008.
45 O. A. Varzatskii, I. N. Denisenko, S. V. Volkov, A. V. Dolganov, A. V. Vologzhanina, Y. N. Bubnov and Y. Z. Voloshin, *Inorg. Chem. Commun.*, 2013, **33**, 147–150.



 